Geophysical Research Letters

RESEARCH LETTER
10.1029/2019GL083039

Special Section:
The Arctic: An AGU Joint Special Collection

Ice Nucleating Particles Carried From Below a Phytoplankton Bloom to the Arctic Atmosphere

J. M. Creamean[1], J. N. Cross[2], R. Pickart[3], L. McRaven[3], P. Lin[3], A. Pacini[3], R. Hanlon[4], D. G. Schmale[4], J. Ceniceros[5], T. Aydell[6], N. Colombi[7], E. Bolger[8], and P. J. DeMott[1]

[1]Department of Atmospheric Science, Colorado State University, Fort Collins, CO, USA, [2]Pacific Marine Environmental Laboratory, National Oceanic and Atmospheric Administration, Seattle, WA, USA, [3]Woods Hole Oceanographic Institution, Woods Hole, MA, USA, [4]School of Plant and Environmental Sciences, Virginia Tech, Blacksburg, VA, USA, [5]Department of Geological Sciences, University of Texas, El Paso, TX, USA, [6]Department of Meteorology and Climate Science, San Jose State University, San Jose, CA, USA, [7]Department of Geography, University of California, Los Angeles, CA, USA, [8]Department of Atmospheric Sciences, University of Miami, Miami, FL, USA

Abstract As Arctic temperatures rise at twice the global rate, sea ice is diminishing more quickly than models can predict. Processes that dictate Arctic cloud formation and impacts on the atmospheric energy budget are poorly understood, yet crucial for evaluating the rapidly changing Arctic. In parallel, warmer temperatures afford conditions favorable for productivity of microorganisms that can effectively serve as ice nucleating particles (INPs). Yet the sources of marine biologically derived INPs remain largely unknown due to limited observations. Here we show, for the first time, how biologically derived INPs were likely transported hundreds of kilometers from deep Bering Strait waters and upwelled to the Arctic Ocean surface to become airborne, a process dependent upon a summertime phytoplankton bloom, bacterial respiration, ocean dynamics, and wind-driven mixing. Given projected enhancement in marine productivity, combined oceanic and atmospheric transport mechanisms may play a crucial role in provision of INPs from blooms to the Arctic atmosphere.

Key Points:
- A persistent phytoplankton bloom in Bering Strait spurred production of microorganisms that produced ice nucleating particles
- Biologically derived ice nucleating particles were vertically transported from the floor to the surface waters of the Arctic Ocean
- Ocean and lower atmosphere dynamics played a key role in transporting and aerosolizing the biologically derived ice nucleating particles

Supporting Information:
- Supporting Information S1

Correspondence to:
J. M. Creamean,
jessie.creamean@colostate.edu

Citation:
Creamean, J. M., Cross, J. N., Pickart, R., McRaven, L., Lin, P., Pacini, A., et al. (2019). Ice nucleating particles carried from below a phytoplankton bloom to the Arctic atmosphere. *Geophysical Research Letters*, *46*, 8572–8581. https://doi.org/10.1029/2019GL083039

Received 27 MAR 2019
Accepted 10 JUL 2019
Accepted article online 15 JUL 2019
Published online 31 JUL 2019

1. Introduction

Arctic mixed-phase clouds (AMPCs) are a key component of the Arctic climate system that affect the delicate energy balance over frozen surfaces (Morrison et al., 2012). One of the least understood processes regarding AMPCs is aerosol-cloud interactions, specifically those pertaining to cloud ice formation by mineral or biological ice nucleating particles (INPs; Solomon et al., 2018). Biologically derived INPs (Bio-INPs; INPs including microbes and their exudates) that form ice greater than −15 °C are typically thought to be of terrestrial origin —yet marine bio-INPs have been shown to form ice at temperatures up to −3 °C (McCluskey et al., 2018a; DeMott et al., 2016; Irish et al., 2017; Irish et al., 2019; Schnell, 1975). AMPC temperatures are often greater than −10 °C on average, are most prevalent in late summer, and can exist down to the surface (Shupe, 2011; Shupe et al., 2006, 2011), while the cloud-driven mixed layer can also extend down to the surface (Shupe et al., 2013). These statistics indicate that marine bio-INPs could play a critical role in cloud formation, especially in the summer when emitted from open water (Wex et al., 2019). Yet field observations of such INPs are exceedingly rare and are mainly reported in midlatitude or Southern Ocean regions (Bigg, 1973; Schnell, 1977).

Measurements of INPs in both the ocean and atmosphere are essential to directly link the thriving marine sources of primary productivity (production of organic matter by phytoplankton) to the clouds above. Schnell (1977) measured INPs in sub-Arctic seawater and air and found cases where atmospheric INPs were comparable or much lower in abundance than those found in the seawater, indicating the ocean was likely the source of the atmospheric INPs. The Arctic summer possesses quintessential conditions for proliferation of primary productivity when open water and daylight hours are at their maxima (Moore et al., 2018). In a recent study, Gabric et al. (2018) demonstrate a clear connection between sea ice extent, productivity, and marine biogenic aerosols. Additionally, recent modeling work has demonstrated that marine organic aerosols lead to increases in cloud ice in polar regions during the summer (Huang et al., 2018). However, to date no studies have reported INP enhancements from naturally occurring phytoplankton blooms, which can

link such sources to the air above. We present results from a summertime expedition in the Bering and Chukchi Seas demonstrating how bio-INPs likely from a phytoplankton bloom became airborne in the lower Arctic atmosphere.

2. Materials and Methods

2.1. Sample Collection

Bulk seawater (herein simply called seawater) and aerosol samples were acquired on the U.S. Coast Guard Cutter *Healy* from 26 August to 13 September 2017 during a collaboration between the Ice Nucleation over the ARCtic Ocean program and the Distributed Biological Observatory (DBO)-Northern Chukchi Integrated Study (Figure 1; Tables S1–S3 in the supporting information). Seawater samples for INPs were collected daily at ~16:00 UTC from *Healy's* underway system intake 8 m below the surface and were analyzed immediately after collection. Seawater samples were also obtained during the occupation of DBO Transect 3 (DBO3; Figure 1(a); Moore & Grebmeier, 2018) for carbon analyses. Sea surface microlayer samples were not collected but have previously been shown to be a rich source of INPs (Abbatt et al., 2019; Irish et al., 2017; Wilson et al., 2015). Daily (24-hr) aerosol samples were collected ~20 m above mean sea level and 8 m from the bow using a time- and size-resolved Davis Rotating-drum Universal-size-cut Monitoring (DRUM) impactor (DA400, DRUMAir, LLC; Creamean et al., 2018a; Creamean et al., 2018b). The DRUM collected aerosol particles at four size ranges (0.15–0.34, 0.34–1.21, 1.21–2.96, and 2.96 to >12 μm in diameter) and sampled at 28.6 L/min. The samples were deposited onto 20 × 190 × 0.05 mm strips of petrolatum-coated perfluoroalkoxy substrate secured onto the rotating drums (20 mm thick, 60 mm in diameter) in each of the four stages at the rate of 7 mm/day (5 mm of sample streaked onto the perfluoroalkoxy substrate followed by 2 mm of blank). Samples were stored at approximately −20 °C for 8–10 months until analysis.

2.2. Ice Nucleation Measurements

The drop-freezing experimentation has previously been described in detail by Creamean et al. (2018a, 2018b) thus is only briefly described here. During testing, the cold plate was cooled variably at 1–10 °C/min from room temperature until around −30 °C. A + 0.33 °C correction factor and uncertainty of ±0.15 °C was added to the probe accuracy uncertainty based on characterization testing presented in Creamean et al. (2018b). A + 2 °C correction factor was added to seawater samples only to account for the typical freezing depression of salt in seawater (Irish et al., 2017; Schnell, 1977). Ultrapure water (Barnstead™ Smart2Pure™) and 30-PSU artificial seawater (Instant Ocean® Sea Salt) blanks were tested to confirm a maximum of a 2 °C freezing point depression. Frozen drops were detected by eye until all 100 drops were frozen (>80% of the freezing temperatures of drops were detected and recorded). Each sample was tested three times with 100 new drops for each test. From the tests, the fraction frozen from detected frozen drops was calculated. Cumulative INP spectra were calculated using the equation by Vali (1971, 2019) and corrected for the total volume of suspension and air per sample. Most seawater samples were subject to heat treatment, which reduces heat-labile INPs that are likely proteinaceous in nature (Hill et al., 2016).

2.3. Oceanographic Measurements

Physical oceanographic measurements were obtained from the underway system in which samples were collected for INP measurements and included, but were not limited to, seawater temperature (SBE3S, Sea-Bird Electronics, Inc.), salinity (SBE21, Sea-Bird Electronics, Inc.), fluorescence (Chlorophyll Fluorometer, Seapoint Sensors, Inc.), partial pressure of carbon dioxide (pCO_2; custom built unit from Palmer Underway pCO_2 system), and dissolved oxygen (dO_2; SBE43, Sea-Bird Electronics, Inc.).

Florescence measurements provided a relative indicator of chlorophyll concentration by scaling a light absorption measurement with a predetermined scale factor (determined by the manufacturer using a monoculture of phytoplankton). Water column measurements from DBO3 were obtained with a conductivity-temperature-depth package consisting of a SBE911-plus (Sea-Bird Electronics, Inc.) for temperature, conductivity, pressure, dO_2, fluorescence, and other parameters not presented herein.

2.4. Biogeochemical Sampling and Analyses

Water samples were taken approximately every 10 m throughout the water column from the conductivity-temperature-depth rosette's 10-L Niskin bottles for total inorganic carbon (TIC), total alkalinity (TA),

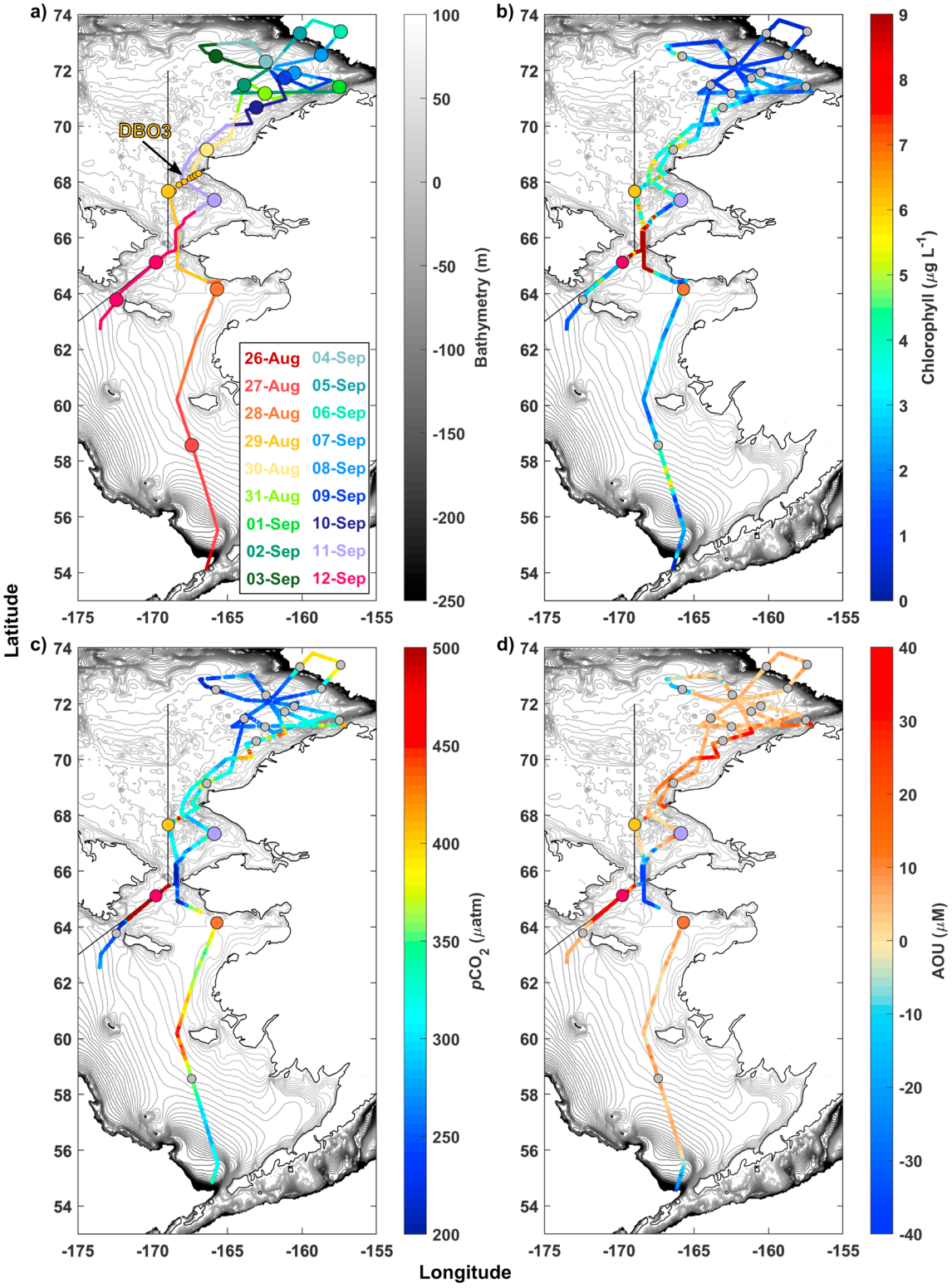

Figure 1. Measurements demonstrating the presence and persistence of the phytoplankton bloom during Ice Nucleation over the ARCtic Ocean program and the Distributed Biological Observatory-Northern Chukchi Integrated Study. The Healy ship track is colored by a date, b chlorophyll, c partial pressure of CO_2 (pCO_2), and d apparent oxygen utilization (AOU). *Mark*ers indicate locations of underway seawater collection. In a, they are colored by date, but only case study samples are colored by date in the other panels while remaining samples are gray. Samples from Distributed Biological Observatory transect 3 (DBO3) are shown in a as small yellow circles. Bathymetry data (0–250 m) were obtained from the USGS publications repository website (https://pubs.usgs.gov/of/2011/1127/ss.html). The thin black line to the west of the ship track represents the U.S./Russian border.

nutrients, and dissolved oxygen. The samples were placed into precleaned ~200-ml borosilicate bottles and poisoned with mercuric chloride to halt biological activity. Samples were analyzed for TIC using an infrared detection system (MARIANDA-AIRICA) and for TA using an open-cell titration system (MARIANDA-VINDTA 3S) according to published best practices for oceanographic CO_2 measurements (Dickson, 2007; Goyet & Snover, 1993). Routine analysis of certified reference material (A.G. Dickson, Scripps Institute of Oceanography) ensured that the accuracy of the TIC and TA measurements averaged 4.3 μmol/kg (~0.2%) and 2.4 μmol/kg (~0.1%), respectively, and were stable over time. pCO_2 was calculated from the bottle temperature and salinity and phosphate, TIC, and TA observations (Robbins et al., 2010). Error in pCO_2 from uncertainty in TA and DIC inputs averaged 15.5 μatm (1.875%). Carbonate dissociation constants from Millero (2006) were applied according to Evans et al. (2015). Error from the use of constants in the calculation of pCO_2 from DIC and TA is estimated to be ±2.7% after Dickson (2010) and Hydes et al. (2010).

2.5. One-Dimensional Ocean Mixing Model

The Price-Weller-Pinkel (PWP; Price et al., 1986) one-dimensional mixing model was utilized to investigate the influence of wind forcing on the stratification of the water column and compute mixed layer depth evolution. It can be forced by surface heat and freshwater fluxes, as well as surface wind stress. In this study, we turned off all forcing except for wind stress and utilized the wind speed time series from *Healy's* meteorological sensors to compute the zonal and meridional components of wind stress. From this, we computed the timescale of deepening of the surface mixed layer.

3. Results and Discussion

3.1. A Robust Bering Strait Bloom

A distinctive phytoplankton bloom near 66°N, 168°W was observed during both transects through Bering Strait (29 August and 12 September 2017) as indicated by enhanced 8-m chlorophyll (up to 32 μg/L)—a proxy for phytoplankton biomass (Figures 1(a) and 1(b); time series in Figure S1). Low pCO_2 and negative apparent oxygen utilization values (Figures 1c and 1d, respectively) were also observed in Bering Strait, indicating uptake of carbon dioxide and oxygen production by phytoplankton, and thus active productivity. Notably, because of the delayed 2016 freezeup in Bering Strait, 2017, was an anomalous year in terms of productivity enhancement and the occurrence of a secondary pulse of production in August, after the primary spring bloom (Figure S2). Secondary blooms are becoming more common because of delayed freezeup and wind-driven mixing in surface waters, not only in Bering Strait but also in regions throughout the Arctic Ocean (Ardyna et al., 2014).

3.2. Anomalous Concentrations of Biological INPs From the Ocean

High concentrations of INPs relative to all seawater samples collected during the cruise were found in the sample collected northwest of the bloom (29 August), where chlorophyll concentrations were relatively low (<5 μg/L; Figure 2a). The 29 August seawater sample represents the upper bounds of what was observed from all samples whereby the entire sample froze before −15 °C. It contained INPs at freezing temperatures warmer than those recently reported from other Arctic locations, but remaining samples had INPs that were comparable to these previous measurements (Figure S3; Irish et al., 2017; Wilson et al., 2015). Heat treatment was used to verify that these INPs contained proteinaceous material and, in fact, that all seawater samples contained such material (Figure S4). Results from supporting Deoxyribonucleic acid (DNA) analysis show there were over twice the number of bacteria in the 29 August sample compared to the 28 August seawater sample (Figure S5). Though we were not able to identify which were responsible for the INPs, the DNA results revealed the presence of known bacterial ice nucleators.

The 29 August coarse-mode aerosol sample followed a similar suit to the seawater, forming ice up to −5 °C (Figure 2b). Furthermore, there were a greater number of viable microorganisms cultured from total aerosol on 29 August compared to 28 August (Figure S6), supporting the fact that the air on 29 August contained relatively high numbers of biological aerosols. The 29 August coarse and total aerosol samples were on the lower end of what has been observed in previous laboratory and field measurements reported in marine boundary layer conditions, but consistent with previous observations in Bering Strait and with what is expected for pristine sea spray (McCluskey et al., 2018b; Figure S7).

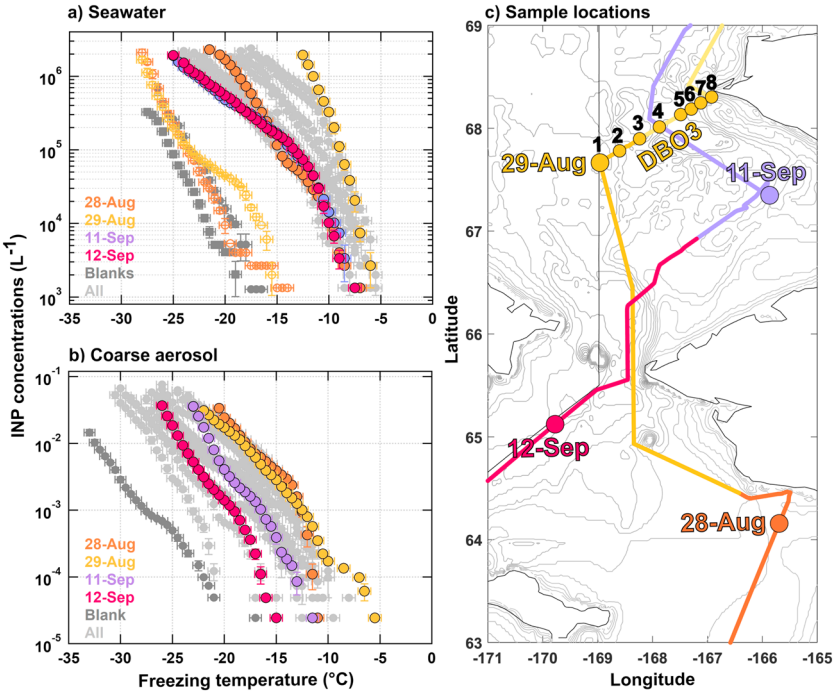

Figure 2. Cumulative ice nucleating particle (INP) concentrations for a seawater and b coarse aerosol samples (for the size ranges of 2.96 to >12 μm). The case study samples are colored by the same schematic as Figure 1a, while spectra from samples collected during remaining, noncase study days are shown in light gray for both seawater and coarse aerosol ("all"). C the map shows the segment of the ship track in Bering Strait where the case study samples were collected. The eight Distributed Biological Observatory transect 3 (DBO3) stations are shown and labeled. The open circles in a represent the heat treated 28 and 29 august seawater samples. The dark gray spectra in a represents the ultrapure water (circles) and 30-PSU artificial seawater (squares) blanks and in b represents the aerosol blank. Error bars for the INP concentrations and freezing temperatures correspond to standard deviation per 0.5 °C bin and temperature probe-plate versus drop variability standard deviation, respectively (Creamean et al., 2018b).

Coarse INPs—at least the lower end of the 3- to 12-μm range—correspond to typical sizes of diatom fragments and bacteria, which are abundant in seawater and therefore more likely to be transferred to aerosol (McCluskey et al., 2018a). Recent studies corroborate our findings whereby INPs are >3 μm in Arctic aerosol (Mason et al., 2016; Si et al., 2018). Bacteria, certain proteins, and cell-free macromolecules fall in the greater than −15 °C INP freezing temperature range (Fröhlich-Nowoisky et al., 2016), whereas most diatoms and phytoplankton typically freeze at temperatures well below this threshold (Knopf et al., 2011). Aerosol compositional information measured during the cruise, air mass transport history, and comparison to previous sea spray studies indicate INPs such as dust were likely not a major source on 29 August and corroborate local marine processes as the prominent source of the INPs (Figures S7 and S8). Combined, key information on previously reported freezing temperatures and particle size and composition indicates the INPs observed in the seawater in the present study were likely bacteria and/or cell-free exudates adhered to larger particles and became aerosolized in the air above the ocean (Wilson et al., 2015).

Historically, the location of the 29 August seawater sample is a "hot spot" for benthic biomass deposition (Grebmeier et al., 2015). In these areas, phytoplankton sink to the bottom, where light limitation and cooler temperatures often favor the proliferation of bacteria. In this hot spot, phytoplankton are deposited on the seafloor due to ocean circulation patterns (Springer et al., 1996), leading to high bacterial abundance north of Bering Strait. The body of previous work in this region demonstrates that the location of the 29 August sample is especially likely to have high bacterial abundance relative to other sampling locations.

3.3. Transport of INPs Caused by Oceanic and Lower Atmospheric Dynamics

Typically, Bering Strait is fed by nutrient-rich Anadyr Water (AW) from the southwest, nutrient-limited Alaskan Coastal Water from the southeast, and Bering Shelf Water directly from the south (Grebmeier, 2012; Grebmeier et al., 2006; Pickart et al., 2010). AW spurs production in the surface waters of Bering

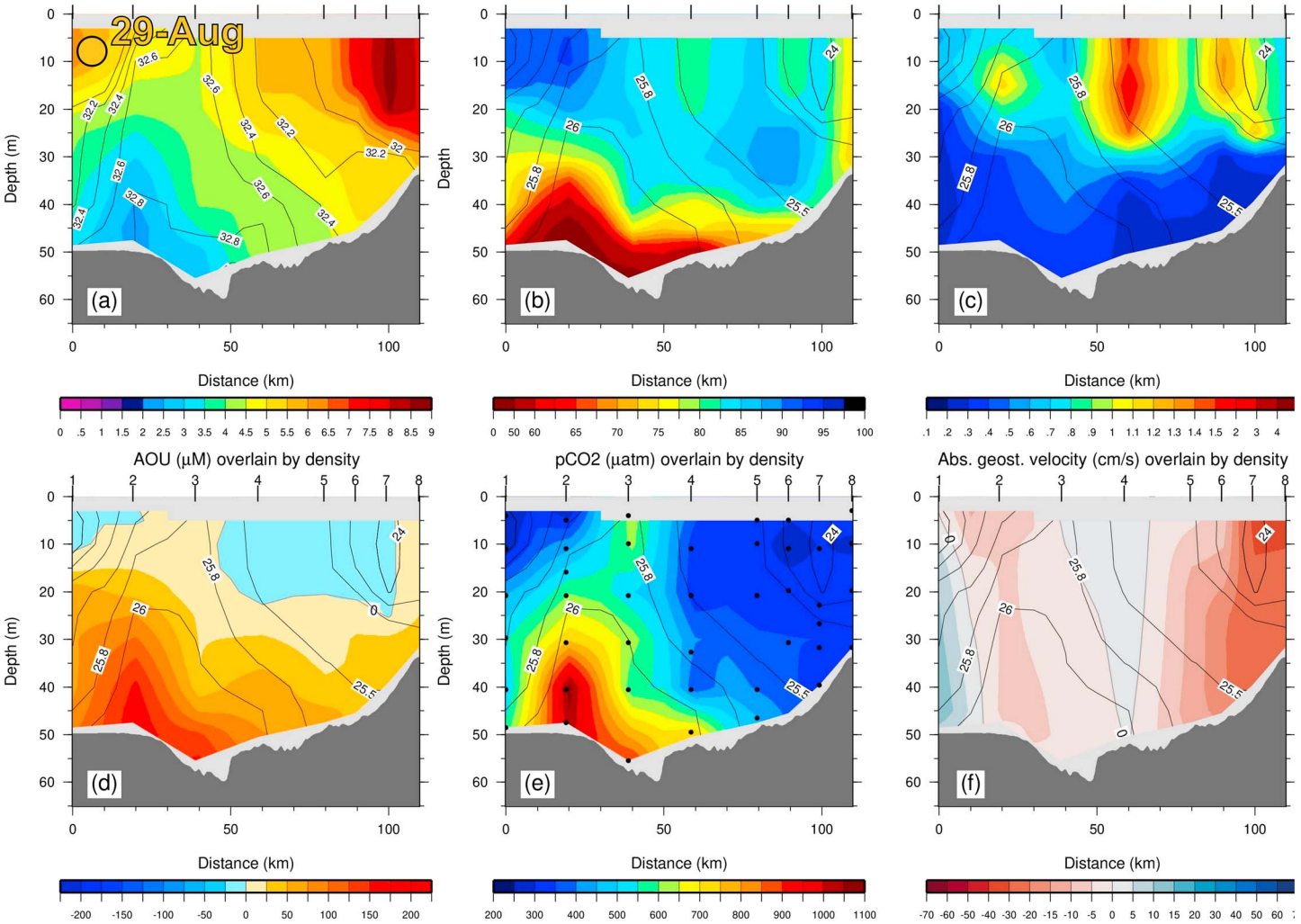

Figure 3. Physical and biogeochemical oceanographic measurements along the Distributed Biological Observatory transect 3 looking to the north. The numbers on the top axes denote the station numbers. The location of the 29 august sample is indicated on panel (a). The bottom depth data are from *Healy's* echosounder. (a) Vertical section of potential temperature (color) overlain by salinity (contours). (b) Same as (a) except for beam transmission (color) overlain by potential density (contours, kg/m^3). (c) Same as (b) except for fluorescence. (d) Same as (b) except for apparent oxygen utilization. (e) Same as (b) except for pCO_2. The water sample data points are marked by the black dots. (f) Same as (b) except for absolute geostrophic velocity. Negative velocities (red shades) are southward.

Strait, and the swift northward flow then carries phytoplankton into the Chukchi Sea. North of the strait, however, the flow weakens considerably (Pisareva et al., 2015), which allows a significant amount of carbon to be exported to the seafloor at the deposition zone where bacterial respiration can occur. The water column measurements from *Healy's* occupation of the DBO3 during 29–30 August suggest that this was the case. The cold and relatively salty AW was prominent near the bottom of Station 2 (Figure 3a). The high turbidity of this water, together with the low fluorescence, positive apparent oxygen utilization, and high pCO_2, indicate active respiration was taking place (Figure 3).

Notably, AW was flowing to the south during the occupation of DBO3 as indicated by absolute geostrophic velocity (Figure 3f). This southward flow, as well as the strong southward flow near the Alaskan coast, was in response to a northerly wind event on the Chukchi shelf that began roughly a week before the occupation of the transect and reached wind speeds exceeding 10 m/s near DBO3 (Figure S9a), which reversed the AW flow. Importantly, however, we verified that the flow through Bering Strait was northward for most of the month of August (Figure S9b). Hence, the bloom activity in Bering Strait likely resulted in deposition of carbon to the seafloor in the region of DBO3 during the time leading up to the cruise, resulting in respiration.

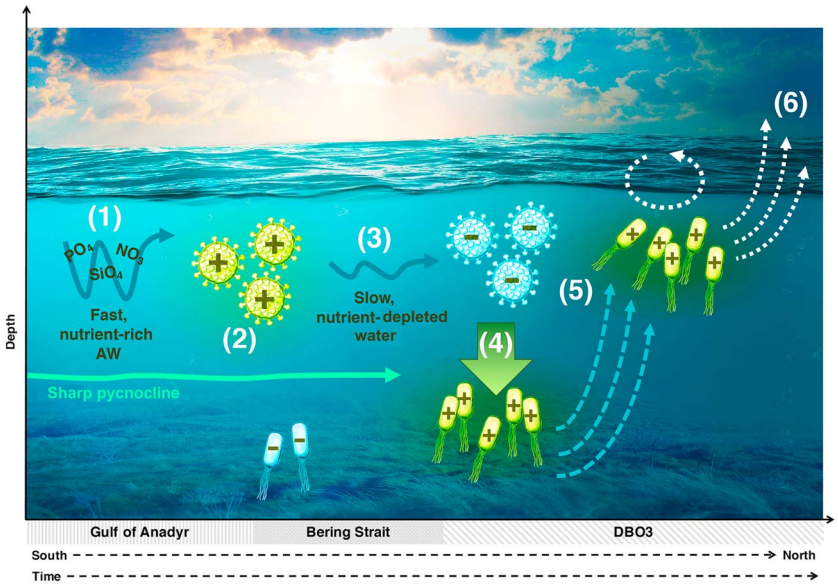

Figure 4. Conceptual model of processes associated with the bloom. Bottom axis represents relative distance and time. Numbers correspond to the steps in the process, namely, (1) nutrient input, (2) primary production, (3) slowing of the current, (4) deposition of nutrient exhaustion, (5) wind-forced turnover, and (6) aerosolization. The blue with the minus sign indicates inactive microbes, while the green with the plus sign indicates actively producing microbes. Blue and white arrows indicate water and air movement, respectively. DBO3 = Distributed Biological Observatory transect 3.

How did the bacteria in the sediments subsequently get transported to the sea surface and released to the atmosphere? We argue that the wind event and the corresponding southward flow in late August were essential to this process. Note the strongly sloped isopycnals (lines of constant density) near Station 2 associated with the southward flow of AW. Just shoreward of this, the 25.8 kg/m^3 isopycnal outcrops at Station 3. This weakly stratified water is more easily homogenized by wind mixing, which might be able to stir material from near the bottom to the sea surface. To test this, we used the PWP model. The density profile of Station 3 was used as the initial condition, and the PWP model was forced with the wind stress associated with the late-August storm. This revealed that the wind-driven surface mixed-layer deepened to within 10 m of the seafloor during the event, which would effectively transport near-bottom material to the sea surface. The mixed-layer depth is commonly observed down to 20–30 m in this region (Rainville et al., 2011).

Another possible mechanism for transporting material from depth to the surface is vertical advection due to convergence in the bottom Ekman layer. On the cyclonic (shoreward) side of the reversed AW jet, the Ekman convergence results in upwelling. A scaling for the vertical velocity is $\zeta H/2$, where ζ is the relative vorticity and H is the bottom boundary layer height (Pedlosky, 1987). Based on the calculated absolute geostrophic velocity, the value of ζ on the cyclonic side of the jet is on the order of 5×10^{-6} s^{-1}. Since the water column is weakly stratified at Station 3, we take H to be on the order of the water depth (50 m). This gives an upwelling rate of ~10 m/day, which means it would take 5 days for water near the bottom to reach the surface. The strong northerly winds began about a week before DBO3 was occupied, implying that the reversed AW jet was present long enough for this to happen. To become airborne, the INPs in the surface waters were then likely aerosolized during ejection from surface bubble bursting, a process which is well known in terms of generating sea spray aerosol (Wilson et al., 2015). The strong wind speeds during the late-August storm likely induced wave breaking and bubble bursting at the surface.

4. Conclusions and Broader Implications

Our results demonstrate that flow dynamics and mixing, in the presence of wind forcing, can strongly impact INP populations from the bottom of the shelf to the air above the surface (Figure 4). Nutrient-rich AW flows into Bering Strait, enabling proliferation of a phytoplankton bloom in the surface waters. The photoinhibited bacteria residing in and near the sediment below the bloom are dormant and unproductive

since vertical export is limited by the rapid lateral transport and food is not available to them. As the flow progresses northward and slows, the nutrients are drawn down, and the phytoplankton starts to decay and sink, providing a steady source of carbon to the seafloor. Bacterial respiration and growth ensue at the deposition zone north of Bering Strait. At this point, northerly wind forcing results in the transport of the active bacteria from the bottom deposition zone to the surface via two mechanisms: upwelling on the cyclonic side of the reversed circulation and turbulent wind mixing. The strong winds also likely induced surface bubble breaking and aerosolization of the bacterial material. Some of these materials were likely proficient INPs that may assist cloud glaciation processes at relatively warm temperatures should they become vertically mixed through the marine boundary layer to cloud levels. Shupe et al. (2006, 2013) report relatively low and warm summertime AMPCs and occasional vertical mixing in the Arctic marine boundary layer, which makes it plausible that the characteristic INPs studied here may reach levels in which they realistically assist cloud glaciation. However, we note that our findings are qualitative in nature and a more quantitative assessment of the relationships between the various measurements should be conducted in future studies.

More broadly, the processes that invigorate AMPC formation are poorly quantified, but results such as ours can help elucidate the sources, abundance, and efficiency of Arctic INPs in addition to the mechanisms that promote aerosolization from the marine environment. One thought-provoking question that arises from this study is as follows: Are shelf deposition zones in the Arctic a key source of airborne INPs? We believe that this question warrants further study, especially considering the ongoing ecological shifts in this region, and potentially other regions, rich in benthic and pelagic activity. Additionally, with the projected increase in Arctic blooms under warmer climate scenarios, quantifying INP abundance and effectiveness from such sources with similar particulate dispersal processes as those reported here is crucial to estimating the Arctic INP and ultimately the Arctic aerosol budget. Another question that should be addressed in future observations is as follows: Will a warmer climate, and thus a more productive Arctic Ocean, serve as a dominant source of INPs that affect AMPC formation? Results from the current work provides motivation to augment the frequency and spatial coverage of targeted Arctic INP, ecological, and oceanographic measurements in the future.

Acknowledgments

We sincerely thank the U.S. Coast Guard and crew of the *Healy* for assistance with equipment installation and guidance, operation of the underway and CTD systems, and general operation of the vessel during transit and at targeted sampling stations. We would also like to thank Allan Bertram, Meng Si, Victoria Irish, and Benjamin Murray for providing INP data from their previous studies. J. M. C., R. P., P. L., L. T., and E. B. were funded by the National Oceanic and Atmospheric Administration (NOAA)'s Arctic Research Program. J. C. was supported by the NOAA Experiential Research & Training Opportunities (NERTO) program. T. A. and N. C. were supported through the NOAA Earnest F. Hollings Scholarship program. A. P. was funded by the National Science Foundation under Grant PLR-1303617. Russel C. Schnell and Michael Spall are acknowledged for insightful discussions during data analysis and interpretation. There are no financial conflicts of interest for any author. INP data are available in the supporting information, while remaining DBO-NCIS data presented in the manuscript are available online (at https://www2.whoi.edu/site/dboncis/).

References

Abbatt, J. P. D., Leaitch, W. R., Aliabadi, A. A., Bertram, A. K., Blanchet, J. P., Boivin-Rioux, A., et al. (2019). Overview paper: New insights into aerosol and climate in the Arctic. *Atmospheric Chemistry and Physics*, *19*(4), 2527–2560. https://doi.org/10.5194/acp-19-2527-2019

Ardyna, M., Babin, M., Gosselin, M., Devred, E., Rainville, L., & Tremblay, J. E. (2014). Recent Arctic Ocean sea ice loss triggers novel fall phytoplankton blooms. *Geophysical Research Letters*, *41*, 6207–6212. https://doi.org/10.1002/2014GL061047

Bigg, E. K. (1973). Ice nucleus concentrations in remote areas. *Journal of the Atmospheric Sciences*, *30*(6), 1153–1157. https://doi.org/10.1175/1520-0469(1973)030<1153:INCIRA>2.0.CO;2

Creamean, J. M., Kirpes, R. M., Pratt, K. A., Spada, N. J., Maahn, M., De Boer, G., et al. (2018a). Marine and terrestrial influences on ice nucleating particles during continuous springtime measurements in an Arctic oilfield location. *Atmospheric Chemistry and Physics*, *18*(24), 18,023–18,042. https://doi.org/10.5194/acp-18-18023-2018

Creamean, J. M., Primm, K. M., Tolbert, M. A., Hall, E. G., Wendell, J., Jordan, A., et al. (2018b). HOVERCAT: A novel aerial system for evaluation of aerosol-cloud interactions. *Atmospheric Measurement Techniques*, *11*(7), 3969–3985. https://doi.org/10.5194/amt-11-3969-2018

DeMott, P. J., Hill, T. C. J., McCluskey, C. S., Prather, K. A., Collins, D. B., Sullivan, R. C., et al. (2016). Sea spray aerosol as a unique source of ice nucleating particles. *Proceedings of the National Academy of Sciences*, *113*(21), 5797–5803. https://doi.org/10.1073/pnas.1514034112

Dickson, A. (2010). Standards for ocean measurements. *Oceanography*, *23*(3), 34–47. https://doi.org/10.5670/oceanog.2010.22

Dickson, A. G. (2007). *Guide to Best Practices for Ocean CO2 Measurements*. PICES Special Publication.

Evans, W., Hales, B., Strutton, P. G., Shearman, R. K., & Barth, J. A. (2015). Failure to bloom: Intense upwelling results in negligible phytoplankton response and prolonged CO_2 outgassing over the Oregon shelf. *Journal of Geophysical Research: Oceans*, *120*, 1446–1461. https://doi.org/10.1002/2014jc010580

Fröhlich-Nowoisky, J., Kampf, C. J., Weber, B., Huffman, J. A., Pöhlker, C., Andreae, M. O., et al. (2016). Bioaerosols in the earth system: Climate, health, and ecosystem interactions. *Atmospheric Research*, *182*, 346–376. https://doi.org/10.1016/j.atmosres.2016.07.018

Gabric, A., Matrai, P., Jones, G., & Middleton, J. (2018). The nexus between sea ice and polar emissions of marine biogenic aerosols. *Bulletin of the American Meteorological Society*, *99*(1), 61–81. https://doi.org/10.1175/BAMS-D-16-0254.1

Goyet, C., & Snover, A. K. (1993). High-accuracy measurements of total dissolved inorganic carbon in the ocean—Comparison of alternate detection methods. *Marine Chemistry*, *44*(2–4), 235–242. https://doi.org/10.1016/0304-4203(93)90205-3

Grebmeier, J., Bluhm, B., Cooper, L., Denisenko, S., Iken, K., Kedra, M., & Serratos, C. (2015). Time-series benthic community composition and biomass and associated environmental characteristics in the Chukchi Sea during the RUSALCA 2004-2012 program. *Oceanography*, *28*(3), 116–133. https://doi.org/10.5670/oceanog.2015.61

Grebmeier, J. M. (2012). Shifting patterns of life in the Pacific Arctic and sub-Arctic seas. *Annual Review of Marine Science*, *4*(1), 63–78. https://doi.org/10.1146/annurev-marine-120710-100926

Grebmeier, J. M., Cooper, L. W., Feder, H. M., & Sirenko, B. I. (2006). Ecosystem dynamics of the Pacific-influenced northern Bering and Chukchi seas in the Amerasian Arctic. *Progress in Oceanography*, *71*(2–4), 331–361. https://doi.org/10.1016/j.pocean.2006.10.001

Hill, T. C. J., DeMott, P. J., Tobo, Y., Fröhlich-Nowoisky, J., Moffett, B. F., Franc, G. D., & Kreidenweis, S. M. (2016). Sources of organic ice nucleating particles in soils. *Atmospheric Chemistry and Physics*, *16*(11), 7195–7211. https://doi.org/10.5194/acp-16-7195-2016

Huang, W. T. K., Ickes, L., Tegen, I., Rinaldi, M., Ceburnis, D., & Lohmann, U. (2018). Global relevance of marine organic aerosol as ice nucleating particles. *Atmospheric Chemistry and Physics*, *18*(15), 11,423–11,445. https://doi.org/10.5194/acp-18-11423-2018

Hydes D. J., Loucaides S., & Tyrrell T. (2010). Report on a desk study to identify likely sources of error in the measurements of carbonate system parameters and related calculations, particularly with respect to coastal waters and ocean acidification experiments. Rep., Research & Consultancy Report 83, National Oceanography Centre, Southampton.

Irish, V. E., Elizondo, P., Chen, J., Chou, C., Charette, J., Lizotte, M., et al. (2017). Ice-nucleating particles in Canadian Arctic Sea-surface microlayer and bulk seawater. *Atmospheric Chemistry and Physics*, *17*(17), 10,583–10,595. https://doi.org/10.5194/acp-17-10583-2017

Irish, V. E., Hanna, S. J., Xi, Y., Boyer, M., Polishchuk, E., Ahmed, M., et al. (2019). Revisiting properties and concentrations of ice-nucleating particles in the sea surface microlayer and bulk seawater in the Canadian Arctic during summer. *Atmospheric Chemistry and Physics*, *19*(11), 7775–7787. https://doi.org/10.5194/acp-19-7775-2019

Knopf, D. A., Alpert, P. A., Wang, B., & Aller, J. Y. (2011). Stimulation of ice nucleation by marine diatoms. *Nature Geoscience*, *4*(2), 88–90. https://doi.org/10.1038/ngeo1037

Mason, R. H., Si, M., Chou, C., Irish, V. E., Dickie, R., Elizondo, P., et al. (2016). Size-resolved measurements of ice-nucleating particles at six locations in North America and one in Europe. *Atmospheric Chemistry and Physics*, *16*(3), 1637–1651. https://doi.org/10.5194/acp-16-1637-2016

McCluskey, C. S., Hill, T. C. J., Sultana, C. M., Laskina, O., Trueblood, J., Santander, M. V., et al. (2018a). A mesocosm double feature: Insights into the chemical makeup of marine ice nucleating particles. *Journal of the Atmospheric Sciences*, *75*(7), 2405–2423. https://doi.org/10.1175/JAS-D-17-0155.1

McCluskey, C. S., Ovadnevaite, J., Rinaldi, M., Atkinson, J., Belosi, F., Ceburnis, D., et al. (2018b). Marine and terrestrial organic ice-nucleating particles in pristine marine to continentally influenced Northeast Atlantic air masses. *Journal of Geophysical Research: Atmospheres*, *123*(11), 6196–6212. https://doi.org/10.1029/2017JD028033

Millero, F. J. (2006). *Chemical Oceanography*. LLC Boca Raton, FL: CRC Press Taylor & Francis Group.

Moore, S. E., & Grebmeier, J. M. (2018). The distributed biological observatory: Linking physics to biology in the Pacific Arctic region + supplementary file (see article tools). *Arctic*, *71*(5). https://doi.org/10.14430/arctic4606

Moore, S. E., Stabeno, P. J., Grebmeier, J. M., & Okkonen, S. R. (2018). The Arctic marine pulses model: Linking annual oceanographic processes to contiguous ecological domains in the Pacific Arctic. *Deep Sea Research Part II: Topical Studies in Oceanography*, *152*, 8–21. https://doi.org/10.1016/j.dsr2.2016.10.011

Morrison, H., de Boer, G., Feingold, G., Harrington, J., Shupe, M. D., & Sulia, K. (2012). Resilience of persistent Arctic mixed-phase clouds. *Nature Geoscience*, *5*(1), 11–17. https://doi.org/10.1038/ngeo1332

Pedlosky, J. (1987). *Geophysical Fluid Dynamics*. New York: Springer-Verlag. https://doi.org/10.1007/978-1-4612-4650-3

Pickart, R. S., Pratt, L. J., Torres, D. J., Whitledge, T. E., Proshutinsky, A. Y., Aagaard, K., et al. (2010). Evolution and dynamics of the flow through herald canyon in the western Chukchi Sea. *Deep Sea Research Part II: Topical Studies in Oceanography*, *57*(1–2), 5–26. https://doi.org/10.1016/j.dsr2.2009.08.002

Pisareva, M. N., Pickart, R. S., Spall, M. A., Nobre, C., Torres, D. J., Moore, G. W. K., & Whitledge, T. E. (2015). Flow of pacific water in the western Chukchi Sea: Results from the 2009 RUSALCA expedition. *Deep Sea Research Part I: Oceanographic Research Papers*, *105*, 53–73. https://doi.org/10.1016/j.dsr.2015.08.011

Price, J. F., Weller, R. A., & Pinkel, R. (1986). Diurnal cycling—Observations and models of the upper ocean response to diurnal heating, cooling, and wind mixing. *Journal of Geophysical Research*, *91*(C7), 8411. https://doi.org/10.1029/JC091iC07p08411

Rainville, L., Lee, C. M., & Woodgate, R. A. (2011). Impact of wind-driven mixing in the Arctic Ocean. *Oceanography*, *24*(3), 136–145. https://doi.org/10.5670/oceanog.2011.65

Robbins, L. L., Hansen M. E., Kleypas J. A., & Meylan S. C. (2010). CO2calc—A user-friendly seawater carbon calculator for Windows, Mac OS X, and iOS (iPhone), 2010–1280 pp, US Geological Survey Open-File Report.

Schnell, R. C. (1975). Ice nuclei produced by laboratory cultured marine phytoplankton. *Geophysical Research Letters*, *2*(11), 500–502. https://doi.org/10.1029/GL002i011p00500

Schnell, R. C. (1977). Ice nuclei in seawater, fog water and marine air off the coast of Nova Scotia: Summer 1975. *Journal of the Atmospheric Sciences*, *34*(8), 1299–1305. https://doi.org/10.1175/1520-0469(1977)034<1299:INISFW>2.0.CO;2

Shupe, M. D. (2011). Clouds at Arctic atmospheric observatories. Part II: Thermodynamic phase characteristics. *Journal of Applied Meteorology and Climatology*, *50*(3), 645–661. https://doi.org/10.1175/2010JAMC2468.1

Shupe, M. D., Matrosov, S. Y., & Uttal, T. (2006). Arctic mixed-phase cloud properties derived from surface-based sensors at SHEBA. *Journal of the Atmospheric Sciences*, *63*(2), 697–711. https://doi.org/10.1175/JAS3659.1

Shupe, M. D., Persson, P. O. G., Brooks, I. M., Tjernstrom, M., Sedlar, J., Mauritsen, T., et al. (2013). Cloud and boundary layer interactions over the Arctic Sea ice in late summer. *Atmospheric Chemistry and Physics*, *13*(18), 9379–9399. https://doi.org/10.5194/acp-13-9379-2013

Shupe, M. D., Walden, V. P., Eloranta, E., Uttal, T., Campbell, J. R., Starkweather, S. M., & Shiobara, M. (2011). Clouds at Arctic atmospheric observatories. Part I: Occurrence and macrophysical properties. *Journal of Applied Meteorology and Climatology*, *50*(3), 626–644. https://doi.org/10.1175/2010JAMC2467.1

Si, M., Irish, V. E., Mason, R. H., Vergara-Temprado, J., Hanna, S. J., Ladino, L. A., et al. (2018). Ice-nucleating ability of aerosol particles and possible sources at three coastal marine sites. *Atmospheric Chemistry and Physics*, *18*(21), 15,669–15,685. https://doi.org/10.5194/acp-18-15669-2018

Solomon, A., de Boer, G., Creamean, J. M., McComiskey, A., Shupe, M. D., Maahn, M., & Cox, C. (2018). The relative impact of cloud condensation nuclei and ice nucleating particle concentrations on phase partitioning in Arctic mixed-phase stratocumulus clouds. *Atmospheric Chemistry and Physics*, *18*(23), 17,047–17,059. https://doi.org/10.5194/acp-18-17047-2018

Springer, A. M., Mcroy, C. P., & Flint, M. V. (1996). The Bering Sea Green Belt: Shelf-edge processes and ecosystem production. *Fisheries Oceanography*, *5*(3–4), 205–223. https://doi.org/10.1111/j.1365-2419.1996.tb00118.x

Vali, G. (1971). Quantitative evaluation of experimental results an the heterogeneous freezing nucleation of supercooled liquids. *Journal of the Atmospheric Sciences*, *28*(3), 402–409. https://doi.org/10.1175/1520-0469(1971)028<0402:QEOERA>2.0.CO;2

Vali, G. (2019). Revisiting the differential freezing nucleus spectra derived from drop-freezing experiments: Methods of calculation, applications, and confidence limits. *Atmospheric Measurement Techniques*, *12*(2), 1219–1231. https://doi.org/10.5194/amt-12-1219-2019

Wex, H., Huang, L., Zhang, W., Hung, H., Traversi, R., Becagli, S., et al. (2019). Annual variability of ice-nucleating particle concentrations at different Arctic locations. *Atmospheric Chemistry and Physics*, *19*(7), 5293–5311. https://doi.org/10.5194/acp-19-5293-2019

Wilson, T. W., Ladino, L. A., Alpert, P. A., Breckels, M. N., Brooks, I. M., Browse, J., et al. (2015). A marine biogenic source of atmospheric ice-nucleating particles. *Nature*, *525*(7568), 234–238. https://doi.org/10.1038/nature14986